

Performance analysis of wireless power transfer using series-to-series topology

Fairul Azhar Abdul Shukor^{1,2}, Ahmed Mohammed Salem Ahmed Alhattami^{1,2}, Nur Ashikin Mohd Nasir^{1,2}, Chockalingam Aravind Vaithilingam^{3,4}

¹Fakulti Kejuruteraan Elektrik, Universiti Teknikal Malaysia Melaka, Melaka, Malaysia

²Electrical Machine Design Research Laboratory, Centre of Robotics and Industrial Automation (CeRIA), Universiti Teknikal Malaysia Melaka, Melaka, Malaysia

³Faculty of Innovation and Technology, Taylor's University, Subang Jaya, Malaysia

⁴Clean Technology Impact Lab, Taylor's University, Subang Jaya, Malaysia

Article Info

Article history:

Received Sep 21, 2022

Revised Dec 16, 2022

Accepted Jan 10, 2023

Keywords:

Finite element method
Inductive power transfer
Wireless power transfer

ABSTRACT

Wireless power transfer (WPT) is a technology used to transmit power using air as its medium of transfer. The function of the WPT is similar to a transformer. The power provided on the primary side will be transferred through air to the secondary side. The performance of the WPT is crucially depends on the air gap length (δ) that separates primary and secondary side. In this paper discusses the performance of WPT using series-to-series topology. The performance of the WPT was estimated using finite element analysis (FEA). During the study, focus was given to effect of turn ratio, a , air gap length and capacitor value at primary (C_p), and secondary, (C_s) winding to voltage ratio of the WPT. The air gap length was set to 1 and 2 mm while the capacitors were set depend on the ratio of primary to secondary winding capacitor (C_p/C_s). The WPT performance also being tested under no-load and loaded operation to observed its effect. As a result, the WPT with turn ratio, a at 0.37, air gap length at 1 mm and ratio of primary to secondary winding capacitor at 0.5 produce the best voltage ratio compared to other settings.

This is an open access article under the [CC BY-SA](https://creativecommons.org/licenses/by-sa/4.0/) license.



Corresponding Author:

Fairul Azhar Abdul Shukor

Fakulti Kejuruteraan Elektrik, Universiti Teknikal Malaysia Melaka

Hang Tuah Jaya, 76100 Durian Tunggal, Melaka, Malaysia

Email: fairul.azhar@utem.edu.my

1. INTRODUCTION

The rise of transfer energy using wireless technology has been accompanied by a sharp increase in the losses in electrical energy. Generally, the wireless power transfer (WPT) is a massive technique for transporting electrical energy from a source to a target load, such as consumer devices, without the need for conductors [1]. Instead of using conventional conductors, the WPT is capable of transporting energy from the power source to the target through the air [2]. Various works have been carried out to analyze, model and characterize the performance of the WPT. Some of them are designed and analyzed the WPT for losses evaluation using experimental [3]. A few researchers intensively studied the series-to-series technology used in the WPT technology. Nevertheless, most of them usually focus on the design optimization of the WPT as hybrid vehicles charging method [4]. The power density evaluation is very important to design a portable WPT that is small, lightweight but transmit high power. In addition, increased number of coils could maximize the delivered voltage to the receiver side of the WPT which could increase power density [5]. However, this research only covered WPT with 2 coils design under near-field application [6].

In industrial applications, usage of the WPT has a huge opportunity. However, its feasibility become challenging especially when involves in complex industrial operation. In consumer application, for example mobile phone, the WPT could solve problem of variation of charging port type from different manufacture. Any devices can be charged using the same WPT device as opposed to having a unique charging cord, hence reduces losses and resources significantly [7]. Moreover, in the realm of electric vehicles, charging it with a wire in public parking lots or at charging stations is the most accessible option for standard charging. Conductive charging for EVs has the disadvantage of having thick gauge cables that are difficult to maintain, present trip hazards, and are susceptible to vandalism [8], [9]. Therefore, the WPT offer to eliminate these concerns, especially in hot environments where the wire used may be severely impacted [10], [11].

The WPT used air as it medium to transmit power. Therefore, the performance of the WPT is depends on the air gap length that separate two side of the WPT. Usually, the higher air gap length (d) the lower power will be transmitted; hence, it is a major factor for the WPT losses [12]. However, by adding a capacitor could create a resonance effect that could improve the WPT performance [13], [14]. These two crucial aspects will be explored and addressed in this research. The primary issue with WPT is power losses, therefore the convenience of not using wires comes at a price. While conduction loss in a conventional copper cable connection is not negligible, losses in WPT are significantly more [15], [16]. A large amount of alternating current is required to generate a magnetic field strong enough to link two separated coils. As known, circulating current in a conducting material result in conduction loss. Consequently, the longer the separation distance between the two coils in WPT, the greater the current required to generate an adequate magnetic field and the higher the system's losses.

2. BASIC CONCEPT OF THE WPT

Currently, the most widely utilized technology for WPT is the inductive coupled WPT (IPT) [17]-[24]. The IPT operates at kHz frequency order and is commonly utilized within a few millimeters to a few centimeters of the target load. The output power capacity of the IPT is in range of few watt until kilowatt depending on transmission efficiency [25]. Magnetic induction is used in IPT, which is a type of near-field wireless power transmission. IPT uses the magnetic field as a medium to transmit power.

The block diagram of a IPT system is as shown in Figure 1. The IPT is energized by using line AC power supply. Usually, the frequency of the line AC power supply is in between 50–60 Hz depending on the standard being used. To allow the power being transmit wirelessly, the frequency of the AC voltage need to be increased up to kHz order. Thus, a power converter will be use for the purpose. The high frequency voltage will be feed into primary side winding before it is being transmitted wirelessly to secondary side winding through magnetic induction method [18]. The frequency then being reduce by using power converter to match with the load requirement.

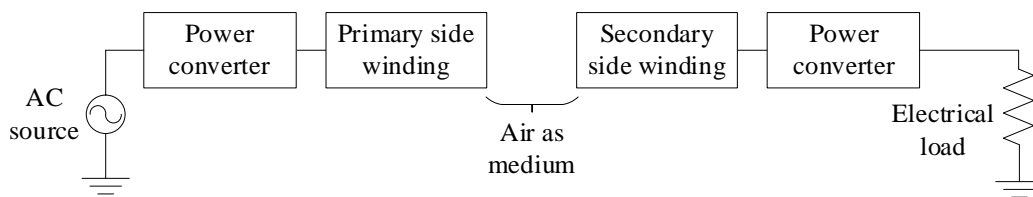


Figure 1. WPT block diagram

The structure and equivalent circuit of the WPT is as shown in Figure 2. The core shape was choose based on the core shape available in the market as shown in Figures 2(a) and (b). The WPT module consists of primary coil, N_p , and secondary coil, N_s . Power supply is connected to the primary side of the coil, while load is connected to the secondary side. The voltage differential between the primary and secondary windings is achieved by adjusting the number of coil turns in the primary winding, N_p , relative to the number of coil turns in the secondary winding, N_s [26]. In this research, the winding turn for primary and secondary windings were varied by varying the copper wire diameter. The copper wire diameter used are as listed in the Table 1. The coil turns and resistance are calculated using (1) and (2).

$$N = \frac{w_c}{\phi_c} \times \frac{h_c}{\phi_c} \times \zeta \quad (1)$$

$$R = \frac{N^2 \rho l_{avg}}{a_{coil}} \quad (2)$$

Where N is the coil turns, w_c is the coil width in m, h_c is the coil height in m, ϕ_c is the copper wire diameter in m, ξ is the winding factor, R is the coil resistance in Ω , ρ is the copper resistivity as $1.68 \times 10^{-8} \Omega m$, l_{ave} is the average length of the copper wire used in m and a_{coil} is the cross sectional area of the coil.

The topology used in this research is series-to-series type as depicted in the equivalent circuit as in Figure 2(c) where all capacitors are connected in series with the primary and secondary winding. Two factor that influence the WPT performance will be investigate which are air gap length (δ) and capacitor ratio (C_p/C_s). The air gap length was set to 1 and 2 mm while the capacitor ratio was set to 0.25, 0.50, 0.75, and 1.00. On top of that, the winding turn for primary and secondary windings were varied too by varying the copper wire diameter. The specification of the WPT is as listed in Table 1.

Once the primary winding is connected a voltage source, it will induce magnetic flux, ϕ . The magnetic flux flows inside the yoke from primary to secondary winding through the air gap. Due to magnetic flux cuts occurred on the secondary winding, a voltage will produce across the secondary winding terminal. The performance of the WPT depends on the air gap length. The lower air gap length set, the lower magnetic resistance on the air gap of the WPT, hence increase the magnetic flux (ϕ) induced by primary winding.

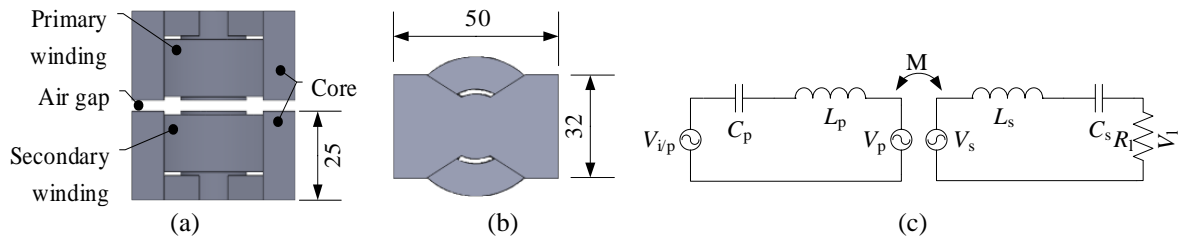


Figure 2. Basic structure and equivalent circuit of the WPT (unit in mm) (a) side view, (b) top view, and (c) equivalent circuit

Table 1. WPT specification

Parameters	Value	Unit
Core outer dimension	50×32×25	mm
Air gap length (δ)	1–2	mm
Copper diameter (ϕ_c)	0.3	mm
Winding turn (N)	1049	384
Winding resistance (R)	12.0	Ω 1.6

3. DESIGN OF THE WPT

Design step of the WPT is as shown in Figure 3. The WPT was designed and simulated under unloaded and loaded conditions. There are 2 models of the WPT has been developed which have air gap length (δ) of 1 mm and 2 mm. Each model of the WPT was set to having different combination of primary, N_p and secondary coil turn, N_s by varying the copper diameter used for the primary (ϕ_{cp}) and secondary, (ϕ_{cs}). Due to fixed dimension of coil width, w_c and height, h_c , the bigger copper diameter (ϕ_c) used, the lesser coil turn obtain. According to the copper diameter (ϕ_c) used for each step, the group of turn ratio, a used is as listed in the Table 2. The group is made based on the same number of turns for primary winding. For this simulation purposes, the voltage supply used is 5 V, 10 kHz. The open voltage was observed for each group of simulation.

Once the unloaded condition is completed, a 1 k Ω pure resistive load is connected on the secondary side terminal to simulate the WPT performance under loaded condition. To create resonance effect on the secondary side, a capacitor, C_s is connected to the secondary side in series with the resistive load. The capacitor on secondary side, C_s is calculated using (3).

$$f = \frac{1}{2\pi R_{load} C_s} \quad (3)$$

Where f is the supply frequency as 10 kHz, R_{load} is the load resistance as 1 k Ω and C_s is the capacitor on the secondary side in F.

Based on the load resistance, R_{load} and supply frequency, f value, the value for the capacitor on the secondary side (C_s) is 16 nF. According to the capacitor ratio (C_p/C_s) set earlier, value for capacitor on primary side (C_p) is as listed in Table 3. Due to the series-series topology selected to be implement, the capacitor on primary side, C_p is also connected in series with the power supply.

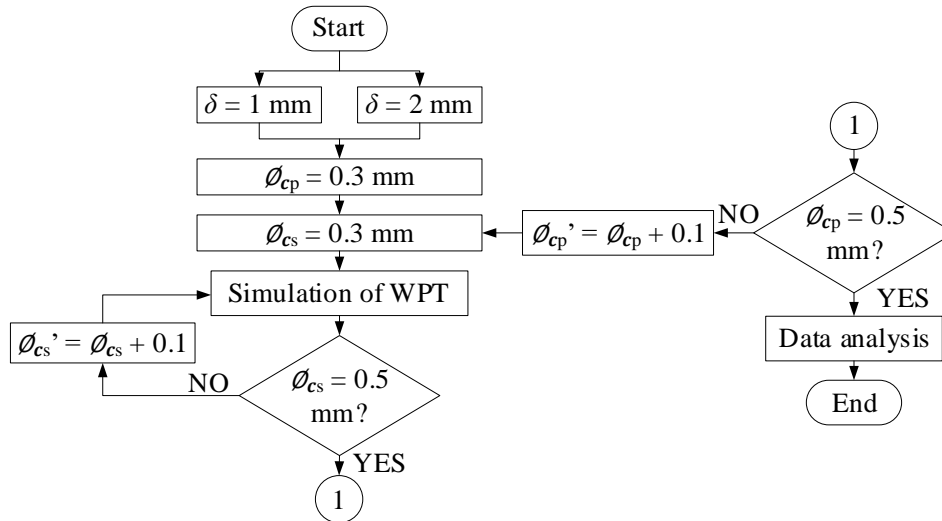


Figure 3. Design of the WPT

Table 2. Turn ratio group

	Case 1	Case 2	Case 3
Group A	$N_p=1,049$ turns $N_s=1,049$ turns $a = N_p / N_s = 1.00$	$N_p=1,049$ turns $N_s=600$ turns $a = N_p / N_s = 1.75$	$N_p=1,049$ turns $N_s=348$ turns $a = N_p / N_s = 2.73$
Group B	$N_p=600$ turns $N_s=1,049$ turns $a = N_p / N_s = 0.57$	$N_p=600$ turns $N_s=600$ turns $a = N_p / N_s = 1.00$	$N_p=600$ turns $N_s=384$ turns $a = N_p / N_s = 1.56$
Group C	$N_p=384$ turns $N_s=1,049$ turns $a = N_p / N_s = 0.37$	$N_p=384$ turns $N_s=600$ turns $a = N_p / N_s = 0.64$	$N_p=384$ turns $N_s=384$ turns $a = N_p / N_s = 1.00$

Table 3. Value of primary and secondary capacitor

C_p/C_s	C_s (nF)	C_p (nF)
0.25	16	4
0.50	16	8
0.75	16	12
1.00	16	16

4. RESULTS AND DISCUSSION

Figure 4 shows sample of the primary (V_p) and secondary, (V_s) voltage waveform under unloaded (Figure 4(a)), loaded without capacitor (Figure 4(b)), and loaded with capacitor (Figure 4(c)) conditions. However, only the unloaded and loaded with capacitor conditions were observed further. Based on the Figures 4(a)-(c), it is shown that, both primary and secondary voltage produce the similar sinusoidal shape. Both primary and secondary voltage were then capture on each different structural and capacitor ratio (C_p/C_s) settings. Then, the peak primary and secondary voltage were acquired and voltage ratio (V_p/V_s) was then calculated and analysed. When the voltage ratio is less 1, it means that the secondary voltage (V_s) produce higher value compared to the primary voltage (V_p). On general application, where the secondary voltage is aimed to be at least the same as the primary voltage, therefore, the configuration of the WPT that produce voltage ratio less than 1 was examined.

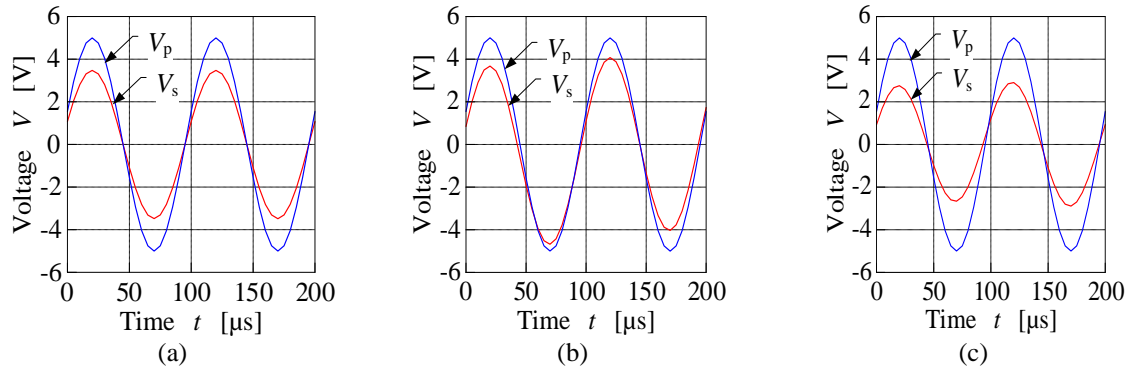


Figure 4. Sample of the WPT output (a) unloaded, (b) loaded without capacitor, and (c) loaded with capacitor

4.1. Unloaded condition performance

Under the unloaded condition, the secondary winding terminal will remain in open circuit. No current flows in the secondary winding, thus, the voltage induced at the secondary winding terminal is not influence by the load and showing the capacity of the secondary winding to induce the secondary voltage. Figure 5 shows the voltage ratio of the WPT under different turn ratio, a and air gap length for unloaded condition. Based on the result, it is shows that, the lower air gap length (δ) the lower the voltage ratio, a produce, hence higher secondary voltage induced. It is because, the lower air gap length the lower magnetic resistance between the primary and secondary core. Therefore, the higher magnetic flux (ψ) will be induced by the primary winding to flows to the secondary winding, thus induced higher voltage at the secondary winding terminal.

For example, under the turn ratio, a of 0.37, the voltage ratio produce are 0.45 and 0.56 for the air gap length of 1 mm and 2 mm respectively. Under this case, the primary (N_p) and secondary (N_s) windings turn are 384 and 1049 respectively. By consideration of the primary voltage (V_p) in this case is 5 V, therefore the secondary voltage, (V_s) induce are 11.11 V and 8.93 V for air gap length of 1 mm and 2 mm respectively.

When the turn ratio, a is increased, the voltage ratio, V_p/V_s is increased too. It is showing the turn ratio, a is direct proportional to the voltage ratio due to similarity of the WPT and a transformer principle. However, unlike the transformer, the relationship between the turn ratio, a and the voltage ratio of the WPT had influenced by a coefficient that represent by slope of the graph. The slope of the graph or can be identified as the slope coefficient, m_c is depends on the air gap length of the WPT. The slope coefficient, m_c is equal to 1.24 and 1.44 at the air gap length of 1 mm and 2 mm respectively. It means that, the higher air gap length used, the higher slope coefficient, m_c produced, hence the lower secondary voltage induced at the same turn ratio (a).

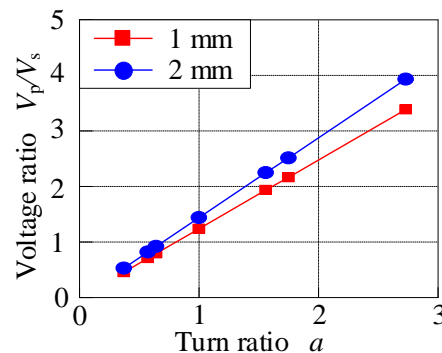


Figure 5. Voltage ratio (V_p/V_s) under different turn ratio, a and air gap length (δ)

4.2. The effect of the capacitor to the secondary voltage (V_s)

When the secondary winding is connected to a load, the voltage induced at its terminal might be influence by the current flows in the load. Generally, the voltage induced will be slightly lower compared to the unloaded condition. However, to improve the voltage induced at the secondary winding terminal, a

capacitor will be connected to the load. The capacitor could be connected in series or parallel depending on the topology used. Since in this paper, the series-to-series topology was focused, therefore the capacitor is connected in series with the load. The load is set to 1 kΩ, the secondary capacitor (C_s) is set to 16 nF and the primary capacitor, C_p is set based on the capacitor ratio (C_p/C_s) between 0.25 to 1.00.

To observe the effect of load and series capacitor to the voltage ratio, the result of relationship between the turn ratio, a and voltage ratio is plot according to turn ratio group. Generally, the higher turn ratio (a) the higher voltage ratio will be for all turn ratio group. On the other hand, by adding capacitor in series with the load, the different of voltage ratio on different air gap length has been reduced. It can be seen by observing the slope coefficient, m_c whereby it is equal to 1.0 and 1.1 for capacitor ratio of 1.00 at air gap length of 1 mm and 2 mm respectively. It can be clearly observed through Figures 6(a)-(f).

On top of that, the slope coefficient, m_c is observing produces different value depending on the capacitor ratio. For example, for the group A and B, at the capacitor ratio of 0.25, the slope coefficient, m_c are about 0.89 and 0.49 respectively at air gap length of 1 mm. For the rest of the slope coefficient, m_c for each condition is as listed in the Table 4.

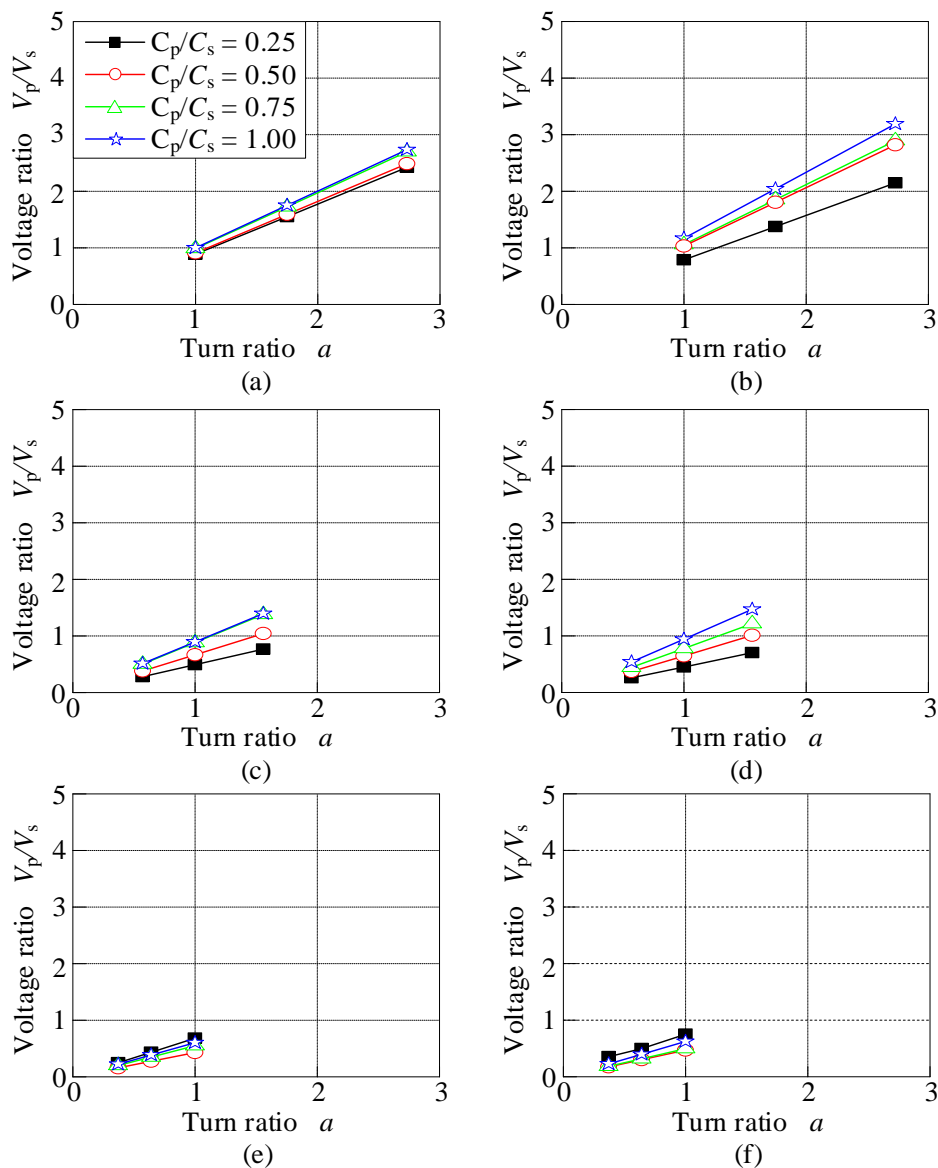


Figure 6. Relationship between turn ratio, a and voltage ratio (V_p/V_s) at different turn ratio group and air gap length, (a) group A $\delta=1$ mm, (b) group A $\delta=2$ mm, (c) group B $\delta=1$ mm, (d) group B $\delta=2$ mm, (e) group C $\delta=1$ mm, and (f) group C $\delta=2$ mm

Table 4. Summary of the WPT performance at turn ratio, a of 0.37

Group	Capacitor ratio, C_p/C_s		Slope coefficient, m_c	
	$\delta=1$ mm	$\delta=2$ mm	$\delta=1$ mm	$\delta=2$ mm
A	0.25	0.89	0.79	
	0.50	0.91	1.03	
	0.75	0.99	1.06	
	1.00	1.00	1.17	
B	0.25	0.49	0.45	
	0.50	0.67	0.65	
	0.75	0.88	0.78	
	1.00	0.90	0.94	
C	0.25	0.68	0.63	
	0.50	0.43	0.48	
	0.75	0.55	0.50	
	1.00	0.61	0.63	

The effect of the capacitors to the voltage ratio (V_p/V_s) of the WPT at specific turn ratio, a is shown in Figures 7(a) and (b). Since the target in this research to obtain higher voltage on the secondary winding terminal, therefore, the voltage ratio with value less than 1 was focused. By comparing the graph plotted in Figures 5 and 7, it is shown that, by adding the capacitor on both sides of the WPT will increased the secondary voltage (V_s). For example, when there is no capacitor added, at the air gap length and turn ratio (a) of 1 mm and 1 respectively, the voltage ratio is 1.24. However, when capacitors were added on the WPT system, at the same settings, the voltage ratio is varied based on the winding turns and capacitor ratio. The lowest voltage ratio is 0.43 at winding turns of 600 and capacitor ratio is 0.5. Meanwhile, the highest voltage ratio is 1.00 at winding turns of 1,049 and capacitor ratio is 1. Therefore, it is found that, the WPT could reach similar or better performance compared to the traditional transformer by adding the capacitors.

Based on overall of the WPT performance, the lowest voltage ratio is obtained at turn ratio, a of 0.37. Table 5 shows comparison the voltage ratio and induced secondary voltage at turn ratio (a) of 0.37 and all capacitor ratio used in this research. Based on the result. The highest secondary voltage could be induced by the WPT is 33.33 V under air gap length of 1 mm and the capacitor ratio (C_p/C_s) of 0.5.

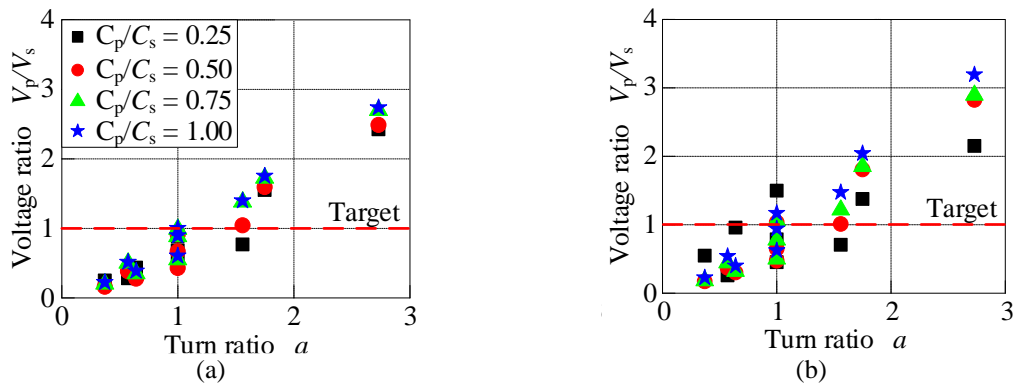


Figure 7. Effect of capacitors to the voltage ratio (V_p/V_s) of the WPT (a) $\delta=1$ mm and (b) $\delta=2$ mm

Table 5. Summary of the WPT performance at turn ratio, a of 0.37

Air gap length (δ) [mm]	Load settings and capacitor ratio (C_p/C_s)	Voltage ratio (V_p/V_s)	Secondary voltage (V_s)[V]	
1	Unloaded	0.45	11.11	
	Loaded	0.25	0.25	20.00
		0.50	0.15	33.33
		0.75	0.20	25.00
		1.00	0.22	22.73
2	Unloaded	0.53	9.43	
	Loaded	0.25	0.35	14.29
		0.50	0.17	29.41
		0.75	0.18	27.78
		1.00	0.23	21.74

5. CONCLUSION

The design and performance comparison of the WPT has been discussed. The aim of this research is to design the WPT hence induce highest as possible secondary voltage. The design settings were considered are the air gap length, turn ratio, a and capacitor ratio were varied. The air gap length was as 1 mm and 2 mm, the turn ratio, a was varied according to copper diameter side used and the capacitor ratio was set to 0.25, 0.50, 0.75, and 1.00. The output of the WPT was observed under 2 operation criteria which are unloaded and loaded condition. Based on the result, it is shows that, the capacitor could increase the voltage induced by the secondary windings. The best voltage ratio was obtained under 1 mm and 0.50 the air gap length and the capacitor ratio. The voltage ratio produce under the settings was 0.15. By considering the primary voltage is 5 V, the secondary voltage is estimated at 33.33 V.

ACKNOWLEDGEMENTS

All authors wishes to acknowledge the Universiti Teknikal Malaysia Melaka (UTeM) for providing financial support to conduct the research and publishing the manuscript.

REFERENCES

- [1] T. S. C. Rao and K. Geetha, "Categories, Standards and Recent Trends in Wireless Power Transfer: A Survey," *Indian Journal of Science and Technology*, vol. 9, no. 20, May 2016, doi: 10.17485/ijst/2016/v9i20/91041.
- [2] M. B. Sidiku, E. M. Eronu, and E. C. Ashigwuike, "A review on wireless power transfer: Concepts, implementations, challenges, and mitigation scheme," *Nigerian Journal of Technology*, vol. 39, no. 4, pp. 1206–1215, Mar. 2021, doi: 10.4314/njt.v39i4.29.
- [3] S. Yana, E. Sinaga, and Fahmi, "Analysis and Design of Wireless Power Transfer," in *Proceedings of the 7th International Conference on Multidisciplinary Research*, 2018, doi: 10.5220/0008882000360040.
- [4] C. Panchal, S. Stegen, and J. Lu, "Review of static and dynamic wireless electric vehicle charging system," *Engineering Science and Technology, an International Journal*, vol. 21, no. 5, pp. 922–937, Oct. 2018, doi: 10.1016/j.jestch.2018.06.015.
- [5] R. Yan, X. Guo, S. Cao, and C. Zhang, "Optimization of output power and transmission efficiency of magnetically coupled resonance wireless power transfer system," *AIP Advances*, vol. 8, no. 5, p. 056625, May 2018, doi: 10.1063/1.5007276.
- [6] A. M. Jawad, R. Nordin, S. K. Gharghan, H. M. Jawad, and M. Ismail, "Opportunities and Challenges for Near-Field Wireless Power Transfer: A Review," *Energies*, vol. 10, no. 7, p. 1022, Jul. 2017, doi: 10.3390/en10071022.
- [7] Q. Li and Y. C. Liang, "An Inductive Power Transfer System With a High-Q Resonant Tank for Mobile Device Charging," *IEEE Transactions on Power Electronics*, vol. 30, no. 11, pp. 6203–6212, Nov. 2015, doi: 10.1109/tpe.2015.2424678.
- [8] Z. Popovic, E. A. Falkenstein, D. Costinett, and R. Zane, "Low-Power Far-Field Wireless Powering for Wireless Sensors," *Proceedings of the IEEE*, vol. 101, no. 6, pp. 1397–1409, Jun. 2013, doi: 10.1109/jproc.2013.2244053.
- [9] S. Assaworrorarit, X. Yu, and S. Fan, "Robust wireless power transfer using a nonlinear parity–time–symmetric circuit," *Nature*, vol. 546, no. 7658, pp. 387–390, Jun. 2017, doi: 10.1038/nature22404.
- [10] C.-S. Wang, O. H. Stielau, and G. A. Covic, "Design Considerations for a Contactless Electric Vehicle Battery Charger," *IEEE Transactions on Industrial Electronics*, vol. 52, no. 5, pp. 1308–1314, Oct. 2005, doi: 10.1109/tie.2005.855672.
- [11] J. Huh, S. W. Lee, W. Y. Lee, G. H. Cho, and C. T. Rim, "Narrow-Width Inductive Power Transfer System for Online Electrical Vehicles," *IEEE Transactions on Power Electronics*, vol. 26, no. 12, pp. 3666–3679, Dec. 2011, doi: 10.1109/tpe.2011.2160972.
- [12] S. Sinha, S. Maji, and K. K. Afridi, "Comparison of Large Air-Gap Inductive and Capacitive Wireless Power Transfer Systems," in *2021 IEEE Applied Power Electronics Conference and Exposition (APEC)*, Jun. 2021, doi: 10.1109/apec42165.2021.9487431.
- [13] Z. Zhang, H. Pang, A. Georgiadis, and C. Cecati, "Wireless Power Transfer—An Overview," *IEEE Transactions on Industrial Electronics*, vol. 66, no. 2, pp. 1044–1058, Feb. 2019, doi: 10.1109/tie.2018.2835378.
- [14] B. Minnaert and N. Stevens, "Maximizing the Power Transfer for a Mixed Inductive and Capacitive Wireless Power Transfer System," in *2018 IEEE Wireless Power Transfer Conference (WPTC)*, Jun. 2018, doi: 10.1109/wptc.2018.8639265.
- [15] Conductix Wampfler Global, "News: Charging electric buses quickly and efficiently: bus stops fitted with modular components make 'Charge & Go' simple to implement," May 13, 2013. <https://www.conductix.com/en/news/2013-05-29/charging-electric-buses-quickly-and-efficiently-bus-stops-fitted-modular-components-make-charge-go> (accessed Jan. 06, 2023).
- [16] B. Olukotun, J. S. Partridge, and R. W. G. Bucknall, "Loss Performance Evaluation of Ferrite-Cored Wireless Power System with Conductive and Magnetic Shields," in *2019 IEEE PES Innovative Smart Grid Technologies Europe (ISGT-Europe)*, Sep. 2019, doi: 10.1109/isgteurope.2019.8905437.
- [17] Z. Kaczmarczyk *et al.*, "Inductive Power Transfer Subsystem for Integrated Motor Drive," *Energies*, vol. 14, no. 5, p. 1412, Mar. 2021, doi: 10.3390/en14051412.
- [18] A. Arshad, S. Khan, A. Z. Alam, and R. Tasnim, "Investigation of inductive coupling approach for non-contact bidirectional transfer of power and signal," in *2012 International Conference on Computer and Communication Engineering (ICCC)*, Jul. 2012, doi: 10.1109/icce.2012.6271251.
- [19] B. Lenaerts and R. Puers, "Inductive powering of a freely moving system," *Sensors and Actuators A: Physical*, vol. 123–124, pp. 522–530, Sep. 2005, doi: 10.1016/j.sna.2005.01.033.
- [20] C. Mkasanga, "A Feasibility Study of Wireless Charging," *Academia.edu*, pp. 1–6.
- [21] X. Lu, P. Wang, D. Niyato, D. I. Kim, and Z. Han, "Wireless Charging Technologies: Fundamentals, Standards, and Network Applications," *IEEE Communications Surveys & Tutorials*, vol. 18, no. 2, pp. 1413–1452, 2016, doi: 10.1109/comst.2015.2499783.
- [22] S. Obayashi, Y. Kanekiyo, and T. Shijo, "UAV/Drone Fast Wireless Charging FRP Frustum Port for 85-kHz 50-V 10-A Inductive Power Transfer," in *2020 IEEE Wireless Power Transfer Conference (WPTC)*, Nov. 2020, doi: 10.1109/wptc48563.2020.9295562.
- [23] Y. Zhang, S. Chen, X. Li, Z. She, F. Zhang, and Y. Tang, "Coil Comparison and Downscaling Principles of Inductive Wireless Power Transfer Systems," in *2020 IEEE PELS Workshop on Emerging Technologies: Wireless Power Transfer (WoW)*, Nov. 2020, doi: 10.1109/wow47795.2020.9291295.

- [24] C. Liu and X. Liu, "Inductive Power Transfer System with Automatic Control," in *2019 IEEE PELS Workshop on Emerging Technologies: Wireless Power Transfer (WoW)*, Jun. 2019, doi: 10.1109/wow45936.2019.9030678.
- [25] T. Helgesen and M. Haddara, "Wireless Power Transfer Solutions for 'Things' in the Internet of Things," in *Proceedings of the Future Technologies Conference (FTC) 2018*, Springer International Publishing, 2018, pp. 92–103, doi: 10.1007/978-3-030-02686-8_8.
- [26] F. Azhar, N. A. M. Nasir, A. L. Hakim, R. N. Firdaus, and A. C. V, "Basic characteristics of wireless power transfer," *Journal of Engineering Science and Technology*, no. 1, pp. 168–178, 2019.

BIOGRAPHIES OF AUTHORS



Fairul Azhar Abdul Shukor     has been a lecturer in Faculty of Electrical Engineering, Universiti Teknikal Melaka Malaysia (UTeM), since 2006. He received his B.Eng. degree and the M.Eng. degree in electrical engineering, from Universiti Putra Malaysia, Malaysia, in 2002 and 2009, respectively; and his Ph.D. degree in Electrical Machine Design from Shinshu University Nagano, Japan, in 2015. He is also a Professional Engineer registered with the Board of Engineers Malaysia (BEM). His research interests include the field of electrical machine design, motor drives, power electronics, and a magnetic sensor. He can be contacted at email: fairul.azhar@utem.edu.my.



Ahmed Mohammed Salem Ahmed Alhattami     received the Engineer degree in Electrical Engineering with honor from University Technical Malaysia Melaka in 2022 with CGPA 3.37 of 4. His Integrated Design Project was monitoring the losses of power in a laboratory circuit, his leadership made the group smoothly achieve all objectives of the project, his final year project (FYP) was in the machine field, studying WPT to explore its use in EVs sector. He pursuing to either work in the machine field to increase and link the theory part of his study to the industry sector or continue a master's degree in EVs, renewable energy, or control strategy for AC machine drive. He can be contacted at email: ahmedalhattami15@gmail.com.



Nur Ashikin Mohd Nasir     is currently a Ph.D candidate in electrical engineering at the Universiti Teknikal Malaysia Melaka (UTeM). She received her B.Eng. Degree in Electrical Engineering (Power Electronics and Drives) and M.Eng. degree in Electrical Engineering from UTeM in 2016 and 2019, respectively. Her research interests include the field of power electronics, motor drives, and electrical machines. She can be contacted at email: nurashikinmohdnasir@gmail.com.



Chockalingam Aravind Vaithilingam     received his Ph.D in Electrical Engineering in 2013 from the University Putra Malaysia, Malaysia. He is the developer of multiple award-winning CODE thinking framework for research and enterprise solutions. He is also heading the Clean Technology Impact Lab addressing UNSDG 6 and UNSDG7 challenges at Taylor's University, Malaysia. He is also a registered Professional Technologists with Malaysian Board of Technologists (MBOT) and registered professional Chartered Engineer with the Engineering Council (UK). He can be contacted at email: chockalingamaravind.vaithilingam@taylors.edu.my.